



Vibrational Spectroscopic Investigations, Conformational Study, Natural Bond Orbital and HOMO-LUMO Analysis of 2-Benzoyl Thiophene

T. CHITHAMBARATHANU^{1,*} and J. DAISY MAGDALINE²

¹Department of Physics, S.T. Hindu College, Nagercoil-629 002, India

²Department of Physics, Rani Anna Government College for Women, Tirunelveli-627 008, India

*Corresponding author: E-mail: tchithambarathanu@gmail.com

Received: 14 April 2015;

Accepted: 21 May 2015;

Published online: 29 August 2015;

AJC-17516

The FTIR and FT-Raman spectra of 2-benzoyl thiophene have been recorded in the region 4000-450 cm⁻¹ and 4000-100 cm⁻¹. The molecular structure, geometry optimization, vibrational frequencies and thermodynamic parameters were calculated using density functional B3LYP method with 6-311++G**basis set. Conformational analysis was performed to find the most stable conformer. The detailed interpretation of the vibrational spectra has been carried out with the aid of normal coordinate analysis based on scaled quantum mechanical force field methodology (SQM). Stability of the molecule arising from hyperconjugative interaction, charge delocalization had been analyzed using natural bond orbital (NBO) analysis. The reactive sites for nucleophilic and electrophilic reactivities were studied from molecular electrostatic potential map. The chemical parameters were calculated using the energy of HOMO and LUMO values. The simulated spectra of the 2-benzoyl thiophene, show excellent agreement with observed spectra or articles.

Keywords: 2-Benzoyl thiophene, Vibrational spectroscopy, Natural bond orbital.

INTRODUCTION

Thiophene belongs to a class of heterocyclic compounds containing a five membered ring made up of one sulphur as heteroatom with the formula C₄H₄S. Thiophene is a unique electron rich heterocycle and has the highest resonance stabilization energy among the five membered heterocycles. The aromaticity in thiophene is attributed to the delocalization of π electrons forming an aromatic sextet in which four electrons are contributed by carbon atoms and a pair of electrons by the sulphur atom in the ring. Thiophene and its derivatives have been emerged as a class of important heterocycles due to the growing abundance of thiophene compounds in natural products, pharmaceuticals and new materials^{1,2}. Thiophene derivatives comprise a significant portion of the organo sulfur compounds in petroleum and in other products from fossil fuels, being obtainable as by-products of petroleum distillation³. Over the years, thiophene derivatives have attracted considerable attention from both medicinal and synthetic chemists due to their utility as versatile intermediates in organic synthesis⁴. Thiophene moiety and its derivatives are structural fragments incorporated in several drugs which possess promising pharmacological characteristics^{5,6}. Thiophene is a common heterocycle for the bioisosteric benzene

replacement in drug development⁷. Thiophenes have diverse biological activities including antimicrobial⁸, antioxidant⁹, antitubercular¹⁰, antidepressant¹¹, analgesic and anti-inflammatory¹², antihypertensive¹³, diabetes mellitus¹⁴, antimetabolite¹⁵, antineoplastic¹⁶, cholesterol inhibition activity¹⁷, anti-allergic¹⁸ and antitumor activities. Thiophene nucleus represents an important toxophore in agrochemistry¹⁹.

Owing to the broad array of applications of thiophene derivatives in the areas of biology, material science and chemistry, an attempt is made to get an insight into the nature of vibrational modes of 2-benzoyl thiophene, a thiophene derivative. In the present work complete vibrational analysis of 2-benzoyl thiophene is performed by combining the experimental and theoretical information using Pulay's density functional theory (DFT) based on scaled quantum chemical approach. The vibrational assignments have been performed based on the potential energy distribution (PED). The redistribution of electron density (ED) in various bonding, antibonding orbitals and E (2) energies have been calculated by natural bond orbital (NBO) analysis to give clear evidence of stabilization originating from the hyper conjugation of various intra molecular interactions. HOMO-LUMO analysis was used to elucidate information regarding charge transfer within the molecule.

EXPERIMENTAL

2-Benzoyl thiophene is purchased from Sigma-Aldrich chemical Company (USA). The FTIR spectra of 2-benzoyl thiophene is recorded using Perkin Elmer RXI spectrometer in the region 4000–450 cm^{-1} with samples in the KBr. The resolution of the spectrum is 4 cm^{-1} . The FT-Raman spectrum of 2-benzoyl thiophene is obtained in the range 4000–100 cm^{-1} using Bruker RFS 100/s FT-Raman spectrophotometer with a 1064 nm Nd: YAG laser source of 150 mW power. The spectral resolution is 2 cm^{-1} .

Computational studies

The molecular structure of 2-benzoyl thiophene and corresponding vibrational harmonic frequencies were calculated using Becke3–Lee–Yang–Parr (B3LYP) with 6-311++G** basis set using GAUSSIAN 03 program package²⁰ without any constraint on the geometry. Normal coordinate analysis has been performed to obtain full description of the molecular motion pertaining to the normal modes. The transformation of force field from Cartesian to internal local-symmetry coordinates, the scaling, the subsequent normal coordinate analysis calculation of total energy distribution (TED) and prediction of IR and Raman intensities are done on a PC with the version V7.0-G77 of the MOLVIB programme written by Sundius^{21,22}. Multiple scaling of the force field has been performed by scaled quantum mechanical force field methodology (SQM) procedure^{23,24} to offset the systematic errors caused by basis set incompleteness, neglect of electron correlation and vibrational anharmonicity. The Raman intensities (S_i) calculated by Gaussian 03 program have been suitably adjusted by the scaling procedure with MOLVIB and subsequently converted to relative Raman intensities (I_i) using the following relationship derived from the basis theory of Raman scattering^{25,26}.

$$I_i = \frac{f(v_o - v_i)^4 S_i}{v_i \left[1 - \exp\left(\frac{-hc v_i}{kT}\right) \right]} \quad (1)$$

where v_o is the exciting frequency (in cm^{-1} units), v_i is the vibrational wave number of the i^{th} mode, h , c , k are universal constants and f is the suitably chosen common scaling factor for all the peak intensities. The simulated IR and Raman spectra have been plotted using with Lorentzian shapes with full width at half maximum (FWHM) of 10 cm^{-1} . Natural bond orbital (NBO) analysis have been performed using natural bond orbital 3.1 program as implemented in the Gaussian 03 W package at the DFT/B3LYP/6-311++G** level of theory. Thermodynamic properties of the title compound at different temperatures have been calculated in gas phase using B3LYP/6-311++G** method. Moreover GaussView 5.0.8 visualization program was utilized to construct the molecular electrostatic potential surface (MEPS), the shape of the highest occupied molecular orbital (HOMO) and the lowest unoccupied molecular orbital (LUMO) orbitals.

RESULTS AND DISCUSSION

Molecular geometry: The structure of the molecules with numbering scheme for the atoms is presented in Fig. 1. The most optimized structural parameters of 2-benzoyl thiophene calculated by DFT/B3LYP level with 6-311++G** basis set

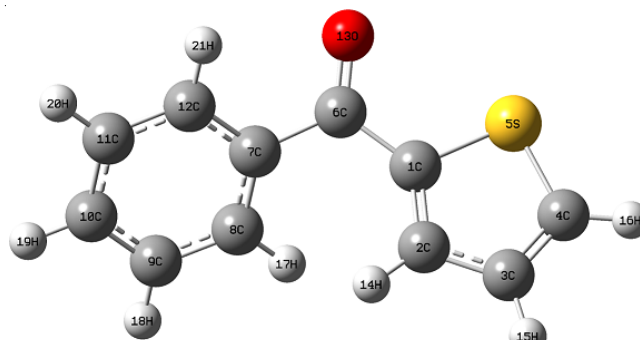


Fig. 1. Optimized structure of 2-benzoyl thiophene at B3LYP/6-311++G** level of theory

were compared with the experimental structure of closely related molecule potassium 3-benzoylthiophene-2-carboxylate available in literature²⁷ and are presented in Table-1. As seen from Table-1, there are small deviations between the calculated and experimental values. It is well known that the experimental results belong to solid phase of molecules, while the theoretical results are related to the gas phase of the isolated molecules. The influence of the substituents on the C-C distances of the ring carbon atoms seems to be small. The C-C bond lengths in the phenyl ring of 2-benzoyl thiophene lie in the range 1.389–1.401 Å while the C-C bond lengths of benzene ring fall in the range 1.379–1.404 Å²⁸. The predicted C-C bond lengths of the thiophene ring in the title compound are also very close to the experimental data of unsubstituted thiophene from experimental works^{29,30}, the maximal difference being 0.04 Å for bond lengths. The C-S bond distance C1-S5 and C4-S5 calculated with DFT/B3LYP are 1.748 and 1.723 Å. These results are in good agreement with those of previously reported for 2-acetyl-5-chlorothiophene and thiophene-2-carbohydrazide^{31,32}. Chaitanya³³, Mahalakshmi and Balachandran³⁴ reported C=O bond length as 1.220, 1.20 Å for the compounds benzophenone 2,4-dicarboxylic acid and 3,3'-bis(trifluoromethyl)-benzophenone. For 2-benzoyl thiophene the C=O bond length is found to be 1.223 Å. The breakdown of the hexagonal and pentagonal symmetry of the phenyl and the thiophene ring due to the conjugation of the carbonyl group with ring π system is confirmed by the widening and contraction of the respective endocyclic angles. The asymmetry of the benzene ring is evident from the deviation of the bond angles at C7, C8, C9, C10, C11 and C12 from the typical hexagonal value 120° as shown in Table-1. More distortion in bond parameters is observed in the hetero aromatic ring than in the benzene ring. The variation in bond angle depends on the electro negativity of the central atom, the presence of lone pair of electrons and the conjugation of the double bonds. For the thiophene ring, the bond angles C2-C1-S5 and C1-C2-C3 (110.78 and 113.20) are found to be appreciably deviated from the reported values for undistorted thiophene (111.47° and 112.43°)^{29,30}. The dihedral angles values S5-C1-C6-C7 (165.98), C2-C1-C6-C7 (-19.33°), C1-C6-C7-C8 (-37.75°) and C1-C6-C7-C12 (145.81°) indicate that the benzene ring and the thiophene ring moieties of the title compound are not planar.

Potential energy scan: The potential energy scan has been performed on 2-benzoyl thiophene at DFT/6-311++G** level with respect to the dihedral angle O13-C6-C1-C2 between 0°

TABLE-1
OPTIMIZED GEOMETRICAL PARAMETERS OF 2-BENZOYL THIOPHENE

Bond length (Å)	B3LYP/6-311++G**	Exp. [Ref. 42]	Bond angle (°)	B3LYP/6-311++G**	Exp. [Ref. 42]	Dihedral angle (°)	B3LYP/6-311++G**	Exp. [Ref. 42]
C1-C2	1.379	1.368	C2-C1-S5	110.78	110.75	S5-C1-C2-C3	-0.72	-0.09
C1-S5	1.748	1.709	C1-C2-C3	113.20	112.90	S5-C1-C2-H14	177.53	
C2-C3	1.418	1.418	C2-C3-C4	112.30	111.96	C6-C1-C2-C3	-175.72	
C3-C4	1.371	1.358	C3-C4-S5	112.44	112.06	C6-C1-C2-H14	2.53	
C4-S5	1.723	1.699	C1-S5-C4	91.27	92.33	C2-C1-S5-C4	0.98	-0.07
C2-H	1.081		C2-C1-C6	130.69		C6-C1-S5-C4	176.67	
C3-H	1.082	0.973	S5-C1-C6	118.36		C2-C1-C6-C7	-19.33	
C4-H	1.080	0.960	C1-C2-H	123.05		C2-C1-C6-O13	159.85	
C1-C6	1.475		C3-C2-H	123.73		S5-C1-C6-C7	165.98	
C6-O13	1.223	1.218	C2-C3-H	124.10	126.65	S5-C1-C6-O13	-14.84	
C7-C8	1.400	1.392	C4-C3-H	123.60	124.83	C1-C2-C3-C4	-0.03	
C7-C12	1.401	1.389	C3-C4-H	128.17	126.65	C1-C2-C3-H15	179.79	
C8-C9	1.394	1.382	S5-C4-H	119.81	121.01	H14-C2-C3-C4	-178.27	
C8-H17	1.083	0.954	C1-C6- C7	119.22		H14-C2-C3- H15	1.55	
C9-C10	1.393	1.371	C1-C6- O13	120.45		C2-C3-C4-S5	0.79	-0.31
C9-H18	1.084	0.919	C7-C6- O13	120.33	120.86	C2-C3-C4-H16	-179.28	174.15
C10-C11	1.396	1.380	C6-C7- C8	122.75	121.25	H15-C3-C4-S5	-179.03	-179.34
C10-H19	1.084	0.945	C6-C7- C12	117.89	119.59	H15-C3-C4- H16	0.90	6.82
C11-C12	1.390	1.379	C8-C7- C12	119.27	119.14	C3-C4-S5-C1	-1.02	0.22
C11-H20	1.084	0.942	C7-C8- C9	120.24	120.28	H16-C4-S5-C1	179.05	174.45
C12-H21	1.083	0.938	C7-C8- H17	120.01	117.96	C1-C6-C7-C8	-37.75	
C6-C7	1.500	1.493	C9-C8- H17	119.72	121.75	C1-C6-C7-C12	145.81	
			C8-C9- C10	120.12	120.03	O13-C6-C7-C8	143.07	169.62
			C8-C9- H18	119.79	124.92	O13-C6-C7-C12	-33.37	11.78
			C10-C9- H18	120.10	114.99	C6-C7-C8-C9	-176.88	178.53
			C9-C10- C11	119.92	120.19	C6-C7-C8- H17	0.98	0.52
			C9-C10- H19	120.02	118.59	C12-C7-C8-C9	-0.48	0.08
			C11-C10- H19	120.06	121.20	C12-C7-C8- H17	177.38	179.13
			C10-C11- C12	120.06	120.33	C6-C7-C12-C11	178.16	177.40
			C10-C11-H20	120.06	118.23	C6-C7-C12-H21	-1.74	-4.27
			C12-C11-H20	119.88	120.99	C8-C7-C12-C11	1.60	-1.18
			C7-C12- C11	120.37	120.02	C8-C7-C12- H21	-178.30	177.10
			C7-C12- H21	118.74	118.13	C7-C8-C9-C10	-0.83	0.92
			C11-C12- H21	120.89	121.84	H17-C8-C9-C10	-178.70	-178.08
						H17-C8-C9- H18	0.98	4.72
						C8-C9-C10-C11	1.04	-0.83
						C8-C9-C10-H19	-179.48	177.49
						H18-C9-C10-C11	-178.63	176.63
						H18-C9-C10- H19	0.85	-5.10
						C9-C10-C11-C12	0.07	-0.27
						C9-C10-C11- H20	179.61	172.10
						H19-C10-C11-C12	-179.41	178.49
						H19-C10-C11- H20	0.13	-6.12
						C10-C11-C12-C7	-1.40	1.28
						C10-C11-C12- H21	178.50	176.93
						H20-C11-C12-C7	179.07	170.88
						H20-C11-C12- H21	-1.04	10.91

and 360° with the increment of 10. The energy curve for rotation of 2-benzoyl thiophene is given in Fig. 2. The PES scan results obtained from DFT as a function of ϕ , shows rotation energy maxima at 90°, 210° and 279° and energy minimum at 10°, 160°, 220° and 360°. The energy profile shows the maximal energy position at 270° (-2356069 kJ mol⁻¹) and the minimal energy position at 160° (-2356097 kJ mol⁻¹) with a small barrier of 28 kJ mol⁻¹. This small energy barrier indicates that the rotation of the entire molecule is not restricted by any group. In addition to this there are two barriers of rotation and the corresponding barriers are 16 and 21 kJ mol⁻¹ respectively.

The torsional profile shows the global minimum (2356097 kJ mol⁻¹) at 160°. This most stable conformer tends to go for a planar conformation with the carbonyl oxygen and the S5 atom in the thiophene ring *syn* position to each other, favouring π delocalization in the molecule. The energy curve also shows local minimum (-2356090 kJ mol⁻¹) at 10 and 350° stabilized by the favourable C12-H21...O13, C2-H14...O13 and C8-H17...S5 hydrogen bonding, with the H21...O13, O13...H14 and H17...S5 bond distances of 2.53 Å, 2.617 Å and 2.732 Å respectively. This S, O *anti* conformation is 7 kJ mol⁻¹ less stable than the S, O *syn*, calculated at the B3LYP/6-311++G** level. As the carbonyl oxygen atom moves closer to the

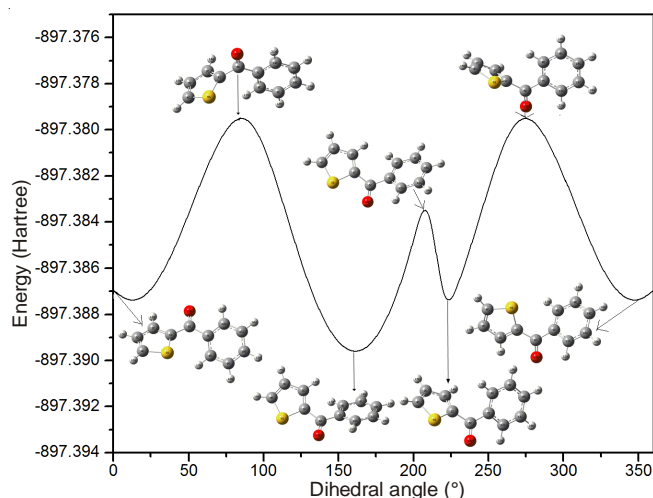


Fig. 2. Potential energy surface scan for the dihedral angle O13-C6-C1-C2

endocyclic S atom the (O13 ...S5 = 2.909 Å) the energy barrier increases and reaches a local energy maximum (-2356079 kJ mol⁻¹) at 210°. The van der Waal's repulsion between H17 and H14 atoms also has significant effect on this barrier.

Vibrational spectral analysis: 2-Benzoyl thiophene molecule consists of 21 atoms and it has 57 fundamental vibrational modes. The vibrational spectral assignments have been carried out with the help of normal coordinate analysis. Non-redundant set of local symmetry coordinates constructed by suitable linear combinations of internal coordinates chosen according to the recommendations of Pulay *et al.*²³ are summarized in Table-2. The computed wave numbers are selectively scaled according to the SQM procedure suggested by Rauhut and Pulay³⁹. The observed and calculated frequencies using B3LYP/6-311++G** basis set along with their relative intensities, probable assignments and potential energy distribution (PED) of 2-benzoyl thiophene are summarized in Table-3. For visual comparison the observed and simulated FT-IR and FT-Raman spectra of the title compound were presented in Figs. 3 and 4.

TABLE-2
DEFINITION OF LOCAL SYMMETRY
COORDINATES OF 2-BENZOYL THIOPHENE

S. No	Symmetry coordinates ^a	Description ^b
1	S ₁ = r _{7,8}	CC stretch
2	S ₂ = r _{8,9}	CC stretch
3	S ₃ = r _{9,10}	CC stretch
4	S ₄ = r _{10,11}	CC stretch
5	S ₅ = r _{11,12}	CC stretch
6	S ₆ = r _{12,7}	CC stretch
7	S ₇ = r _{4,3}	CC stretch
8	S ₈ = r _{2,1}	CC stretch
9	S ₉ = r _{3,2}	CC stretch
10	S ₁₀ = r _{7,6}	CC stretch
11	S ₁₁ = r _{1,6}	CC stretch
12	S ₁₂ = r _{4,5}	CS stretch
13	S ₁₃ = r _{1,5}	CS stretch
14	S ₁₄ = r _{6,13}	CO stretch
15	S ₁₅ = r _{3,15}	CH stretch
16	S ₁₆ = r _{4,16}	CH stretch
17	S ₁₇ = r _{2,14}	CH stretch
18	S ₁₈ = r _{8,17}	CH stretch

19	S ₁₉ = r _{9,18}	CH stretch
20	S ₂₀ = r _{10,19}	CH stretch
21	S ₂₁ = r _{11,20}	CH stretch
22	S ₂₂ = r _{12,21}	CH stretch
23	S ₂₃ = β _{7,8,17} - β _{9,8,17}	CH deformation
24	S ₂₄ = β _{8,9,18} - β _{10,9,18}	CH deformation
25	S ₂₅ = β _{9,10,19} - β _{11,10,19}	CH deformation
26	S ₂₆ = β _{10,11,20} - β _{12,11,20}	CH deformation
27	S ₂₇ = β _{11,12,21} - β _{7,12,21}	CH deformation
28	S ₂₈ = β _{1,2,14} - β _{3,2,14}	CH deformation
29	S ₂₉ = β _{2,3,15} - β _{4,3,15}	CH deformation
30	S ₃₀ = β _{3,4,16} - β _{5,4,16}	CC deformation
31	S ₃₁ = β _{12,7,6} - β _{8,7,6}	CC deformation
32	S ₃₂ = β _{2,1,6} - β _{5,1,6}	CH deformation
33	S ₃₃ = β _{9,8,7} - β _{8,7,12} + β _{7,12,11} - β _{12,11,10} + β _{11,10,9} - β _{10,9,8}	Ring 1 deformation
34	S ₃₄ = 2β _{9,8,7} - β _{8,7,12} - β _{7,12,11} + 2β _{12,11,10} - β _{11,10,9} - β _{10,9,8}	Ring 1 deformation
35	S ₃₅ = β _{8,7,12} - β _{7,12,11} + β _{5,4,3} - β _{11,10,9} - β _{10,9,8}	Ring 1 deformation
36	S ₃₆ = β _{4,5,1} + a(β _{5,1,2} + β _{3,4,5}) + b(β _{1,2,3} + β _{2,3,4})	Ring 2 deformation
37	S ₃₇ = (a-b)(β _{5,1,2} - β _{3,4,5}) + (1-a)(β _{1,2,3} - β _{2,3,4})	Ring 2 deformation
38	S ₃₈ = 2β _{7,6,1} - β _{7,6,13} - β _{1,6,13}	CCC deformation
39	S ₃₉ = β _{7,6,13} - β _{1,6,13}	CO deformation
40	S ₄₀ = γ _{21,12,7,11}	CH wag
41	S ₄₁ = γ _{20,11,10,12}	CH wag
42	S ₄₂ = γ _{19,10,9,11}	CH wag
43	S ₄₃ = γ _{17,8,7,9}	CH wag
44	S ₄₄ = γ _{18,9,8,10}	CH wag
45	S ₄₅ = γ _{14,2,1,3}	CH wag
46	S ₄₆ = γ _{15,3,2,4}	CH wag
47	S ₄₇ = γ _{16,4,5,3}	CH wag
48	S ₄₈ = γ _{6,1,5,2}	CC wag
49	S ₄₉ = γ _{6,7,8,12}	CC wag
50	S ₅₀ = γ _{13,6,7,1}	CC wag
51	S ₅₁ = γ _{8,7,12} - γ _{8,7,12,11} + γ _{7,12,11,10} - γ _{12,11,10,9} + γ _{11,10,9,8} - γ _{10,9,8,7}	Ring 1 torsion
52	S ₅₂ = 2γ _{9,8,7,12} - γ _{8,7,12,11} - γ _{7,12,11,10} + 2γ _{12,11,10,9} - γ _{11,10,9,8} - γ _{10,9,8,7}	Ring 1 torsion
53	S ₅₃ = γ _{8,7,12,11} - γ _{7,12,11,10} + γ _{11,10,9,8} - γ _{10,9,8,7}	Ring 1 torsion
54	S ₅₄ = b(γ _{4,5,1,2} + γ _{3,4,5,1}) + a(γ _{5,1,2,3} + γ _{2,3,4,5}) + γ _{1,2,3,4}	Ring 2 torsion
55	S ₅₅ = (a-b)(γ _{2,3,4,5} - γ _{5,1,2,3}) + (1-a)(γ _{3,4,5,1} + γ _{4,5,1,2})	Ring 2 torsion
56	S ₅₆ = τ _{12,7,6,13} + τ _{8,7,6,13}	CC torsion
57	S ₅₇ = τ _{2,1,6,13} + τ _{5,1,6,13}	CC torsion

Atom numbering as in Fig. 5.

^aDefinitions are made in terms of the standard valence coordinates: r_{i,j} is the bond length between atoms i and j; β_{ijk} is the valence angle between i,j,k where j is the central atom; γ_{ijkl} is the out-of-plane angle between the i-j bond and the plane defined by the j,k,l atoms; τ_{ijkl} is the torsion (dihedral) angle between the plane defined by I,j,k and j,k,l atoms: a = cos 144° and b = cos 72°

Thiophene ring vibrations: The hetero aromatic structure shows the presence of C-H stretching vibrations in the region 3100–3000 cm⁻¹, which is the characteristic region for the ready identification of carbon–hydrogen stretching vibrations³⁵. In this region, the bands are not affected appreciably by the nature of substituents. According to Socrates, thiophenes absorb at 3100–3000 cm⁻¹ due to the C-H stretching vibrations³⁶. Sert *et al.*³⁷ observed C-H vibrations of *tert*-butyl-N-(thiophene-2-yl)carbamate at 3125, 3093 and 3068 cm⁻¹ in the FT-IR spectrum. For 2-acetyl-5-chlorothiophene Chidan Kumar *et al.*³² assigned C-H stretching frequencies at 3146 and 3103 cm⁻¹ in the IR

TABLE-3
 ASSIGNMENTS OF FUNDAMENTAL VIBRATIONS OF 2-BENZOYL THIOPHENE BY
 NORMAL COORDINATE ANALYSIS BASED ON SQM FORCE FIELD CALCULATIONS

S. No.	Observed wavenumbers (cm ⁻¹)		Selectively scaled B3LYP/6-311++G** force Field			
	IR	Raman	v _i (cm ⁻¹)	IR ^a	R ^b	Assignment with potential energy distribution (%) ^c
1		3131	3130	0.44	229.04	vCH(99)
2		3110	3113	0.78	67.60	vCH(99)
3	3096	3097	3095	5.32	104.90	vCH(99)
4	3074		3071	7.09	235.10	vCH(99)
5			3067	8.80	70.91	vCH(99)
6		3061	3059	16.59	100.03	vCH(99)
7	3050		3048	7.72	124.98	vCH(99)
8	3027	3027	3039	0.07	44.57	vCH(99)
9	1627	1625	1631	207.86	165.70	vC=O(65), vCC(12)
10	1591	1596	1585	14.27	150.11	vCC(66), βCH(21)
11	1572		1565	32.35	29.47	vCC(60), βCH(18)
12	1513		1524	25.01	4.32	vCC5(72), βCH5(18)
13		1480	1468	0.08	4.58	β CH(61), vCC(34)
14	1448		1438	26.93	0.94	β CH(51), vCC(39)
15	1412	1414	1411	70.76	17.72	vCC5(89), βCH5(10)
16	1349	1352	1336	5.07	7.76	vCC5(64), β CH5(19)
17	1316		1314	24.27	3.89	β CH(83)
18	1286	1289	1299	23.09	1.91	vCC(86)
19	1228	1231	1255	265.58	12.24	vCC _{ar} (46), vCC(13), βOC(13)
20	1178	1184	1199	29.69	8.85	βCH5(77)
21		1166	1161	12.41	2.26	βCH(77), vCC(21)
22	1135	1138	1144	0.22	5.02	βCH(80), vCC(20)
23	1105		1105	12.60	56.00	vCC _{ar} (25), vCC5(20), βR1(17), βCH(10), vCS(10),
24	1077	1080	1072	11.87	2.46	βCH(47), vCC(43)
25	1050	1056	1052	2.61	15.53	βCH5(84), vCC5(11)
26	1022	1027	1028	30.38	2.05	βCH5(45), vCC5(30), vCC(10),
27		1014	1014	19.54	15.16	vCC(44), β R1(29), βCH(15),
28	998	999	989	0.55	71.15	vCC(51), βR1(46)
29	977	983	965	0.29	0.19	γCH(82), τR1(17)
30	940	942	949	2.20	0.29	γCH(92)
31	919	921	918	5.22	1.51	γCH(72), τR1(12)
32	878		888	0.60	0.73	βCH5(88)
33		861	854	46.31	5.09	OCroc(28), vCS(16), vCC(11),
34	838	840	837	23.71	10.11	vCS(86), βR2(13)
35			828	3.59	2.86	γCH5(60), γCH(27)
36		817	820	5.76	0.96	γCH(69), γCH5(27)
37	793		783	3.08	7.49	γCH(26), γCC _{ar} (18), τR1(18)
38	717		718	7.86	19.95	vCS(52), βR2(21)
39		706	699	64.05	0.35	βCH5(99)
40		686	690	58.26	3.37	γCH(45), γOC(16), βR2(13)
41		668	678	45.77	3.91	γCH(38), βR1(18), βR2(15), τR1(11)
42	643	649	656	10.23	1.25	τR1(67), γCH(13)
43			624	5.39	7.92	βR1(34), βR2(30)
44		616	618	1.62	5.41	βR1(66), βR2(12)
45	564		566	1.52	0.99	τR2(87)
46	538	539	538	1.30	2.71	τR1(21), βR2(17), βCCC(14)
47	455		453	1.26	0.37	τR2(71), γCCar(14)
48		410	419	2.94	0.41	τR1(44), γCCar(19)
49		396	390	0.46	1.80	τR1(82), γCH(16)
50		375	368	1.61	0.88	τR1(18), OCroc(18), vCC _{ar} (15), βR2(12), βR2(11)
51		279	271	1.65	1.26	βCC _{ar} (12), vCC _{ar} (20), βR2 _r (12)
52		236	234	1.56	1.46	βCC _{ar} (26), βCC _{ar} (14), vCC _{ar} (10)
53		206	205	1.40	2.95	β5CC _{ar} (41), τR1(21)
54		131	132	1.00	1.34	γCC5ar(32), τCC(25), τCC1(18)
55		101	98	1.03	4.57	βCCC(24), τR1(20), γCC5ar(18), γCC(18)
56			59	0.15	6.11	τCC(55) βCCC(16),
57			45	1.57	1.16	τCC1(89)

(v) stretching; (β) in-plane-bending; (γ) out-of-plane-bending; (δ) scissoring; (τ) torsion; ^aCalculated IR intensities; ^bRaman activity; ^cOnly potential energy distribution values greater than 10 % are given.

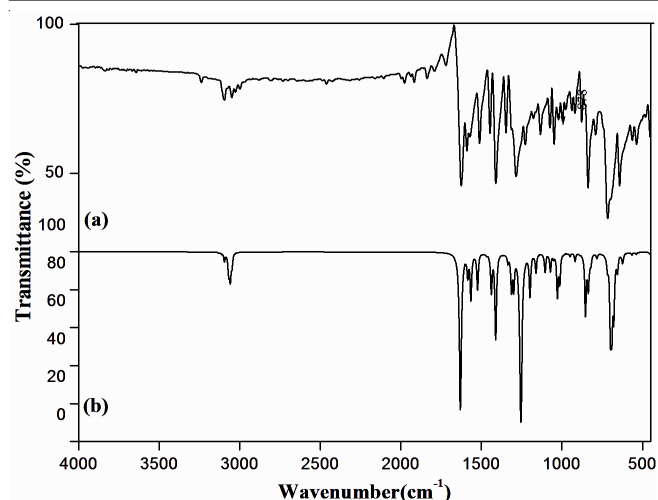


Fig. 3. Experimental (a) and (b) simulated FTIR spectra of 2-benzoyl thiophene

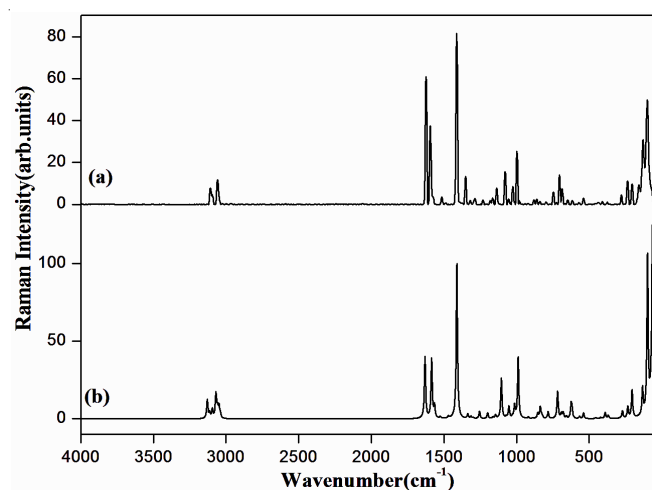


Fig. 4. Experimental (a) and (b) simulated FT Raman spectra of 2-benzoyl thiophene

spectra. For the title compound the bands observed at 3096 cm^{-1} in the IR spectrum and at 3131, 3110, 3097 cm^{-1} in the Raman spectrum and at 3130, 3113, 3095 cm^{-1} theoretically are assigned to C-H stretching mode. In the aromatic five-membered ring heterocycles the in-plane and out-of plane C-H bending vibrations appear in the range³⁸ 1300–1000 cm^{-1} and 1000–700 cm^{-1} . The C-H in plane bending modes with weak to moderate intensity are observed in the IR of 2-benzoyl thiophene at 1178, 1050 and 1022 cm^{-1} and the Raman frequencies are observed at 1184 and 1027 cm^{-1} . The calculated wavenumbers for this mode are 1199, 1052 and 1028 cm^{-1} . The out-of-plane bending vibrations of the title molecule are assigned to the bands at 878, 706 cm^{-1} in the IR spectrum which shows good agreement with the predicted DFT values at 888, 827, 699 cm^{-1} respectively. The aromatic ring stretching vibrations occur generally in the region 1600–1350 cm^{-1} . The position and the intensity of the ring stretching bands of aromatic five membered ring hetero cycles are more sensitive than the corresponding bands of benzene to changes in the substituents so that wide frequency variation can occur, exceptionally in thiophene which involves the movement of the heavy sulphur heteroatom³⁹. For 2 substituted thiophenes,

these bands are observed at 1532–1514, 1454–1430 and 1367–1347 cm^{-1} from the wavenumber ranges given by Rao for the three bands in the region. Sert *et al.*³⁷ assigned the bands 1563, 1500, 1449, 1221, 1027 to the ring stretching modes of the thiophene ring. Karaback *et al.*⁴⁰ reported these modes at 1514, 1405, 1358 cm^{-1} in the IR spectrum and at 1515, 1403 cm^{-1} in the Raman spectrum. In the present investigation the carbon-carbon stretching vibrations calculated at 1524, 1414 and 1336 cm^{-1} show good agreement with the experimental infrared bands at 1513, 1412 and 1349 cm^{-1} and Raman bands at 1414 and 1352 cm^{-1} . Small changes in the wavenumber observed for these modes are due to the change in force constants/reduced mass ratio resulting mainly from the extent of mixing between ring and substituent group. The C-S stretching frequency generally appears as a band of weak and moderate intensity in the range 720–570 cm^{-1} . The difficulty experienced in recognizing this band is due to the presence of the intense C-H out-of-plane deformation in this region. The stretching of the C-S bond in the thiophene ring of 2-benzoyl thiophene appears as a strong bands at 838 and 717 cm^{-1} in infrared. The C-S vibrations are computed at 837 and 718 cm^{-1} by DFT/B3LYP with a potential energy distribution of ~50 %. These assignments agree well with those reported for other thiophene compounds^{31,32, 37,40,41}.

C=O vibrations: The carbonyl group is very important in infrared spectrum because of its strong intensity of absorption and high sensitivity towards relatively minor changes in its environment. Conjugation, ring size, hydrogen bonding and electronic effects often result in significant shifts in C=O absorption frequencies^{36,38}. The intensity of these bands can increase because of conjugation, leading to the intensification of the Raman lines as well as increase in infrared band intensities. Carbonyl compounds give rise to strong band in the region 1900–1500 cm^{-1} due to stretching of the C=O bond. Doubly conjugated ketones, quinones and benzophenones usually absorb near⁴² 1680–1640 cm^{-1} . If a carbonyl group is part of a conjugated system, then the frequency of the carbonyl stretching frequency decreases, because of the decrease in the double bond character of the C=O group due to the delocalization of the π electron system³⁶. In benzophenone⁴³, the sharp intense band in the Raman spectrum at 1650 cm^{-1} is assigned to the C=O stretching mode. Mahalakshmi and Balachandran⁴⁴ observed C=O stretching at 1654 cm^{-1} in FT-IR and 1675 cm^{-1} in FT-Raman for 3,3'-bis(trifluoromethyl)benzophenone and Vainia *et al.*⁴⁵ assigned C=O stretching bands at 1636 cm^{-1} for 4-Hydroxy-2,5-dimethylphenyl-benzophenone. This mode for 2-benzoyl thiophene appears at 1627 cm^{-1} in the IR spectrum and 1625 cm^{-1} in the Raman spectrum as very strong bands. The DFT calculations give this mode at 1625 cm^{-1} .

Phenyl ring vibrations: Aromatic compounds commonly exhibit multiple weak bands in the region 3100–3000 cm^{-1} due to aromatic C-H stretching vibration³⁵. In 2-benzoyl thiophene, the C-H stretching vibrations are observed at 3074, 3050 and 3027 cm^{-1} in FTIR spectrum and at 3061 and 3027 cm^{-1} in FT-Raman spectrum. The theoretically calculated values are 3071, 3067, 3059, 3048, 3039 cm^{-1} . As indicated by the potential energy distribution, these five modes involve above 95 % contribution suggesting that they are pure

stretching modes. The aromatic C-H in-plane bending modes of benzene and its derivatives are observed in the region 1300–1000 cm^{-1} . The IR bands corresponding to these modes are sharp but have weak-to-medium intensity and in Raman spectra these vibrations are very useful for characterization purposes and are strong³⁶. The C-H in-plane bending vibrations calculated at 1315, 1161, 1149, 1077 cm^{-1} are assigned to the FTIR bands at 1316, 1135, 1077 cm^{-1} and FT-Raman bands at 1165, 1138 and 1080 cm^{-1} . The aromatic C-H in-plane bending vibrations have substantial overlapping with the ring C-C stretching vibrations. The absorption bands arising from C-H out-of-plane bending vibrations are usually observed in the region^{35,36,42,46} at 1000–675 cm^{-1} . The C-H in-plane bending modes observed in the FTIR spectrum of 2-benzoyl thiophene at 977, 940, 919 and 793 cm^{-1} and in the FT-Raman spectrum at 983, 942, 921, 901, 706 and 668 cm^{-1} show good agreement with the theoretically scaled harmonic wavenumber values. The ring C=C and C-C stretching vibrations, known as semicircle stretching, usually occur in the region³⁵ 1625–1400 cm^{-1} . The benzene ring possesses six stretching vibrations of which the four with the highest wavenumbers occurring near 1600, 1580, 1490 and 1440 cm^{-1} are good group vibrations. With heavy substituents the bands tend to shift to lower wavenumbers. The fifth ring stretching vibration is active near $1315 \pm 65 \text{ cm}^{-1}$ and the sixth stretching or ring breathing mode appears as a weak band⁴⁶ near 1000 cm^{-1} . For the benzene ring in 2-benzoyl thiophene molecule, the prominent peaks at 1591, 1572, 1448, 1286 cm^{-1} in FTIR and peaks at 1596, 1289 cm^{-1} in FT-Raman are due to C-C stretching vibration. For the title compound the ring breathing vibration appears as a medium strong band at 999 cm^{-1} in the Raman spectrum, as a weak band at 998 cm^{-1} in the IR spectrum and the theoretically calculated value is at 989 cm^{-1} . The ring breathing band is reported at about 1003 and 998 cm^{-1} by Viania *et al.*⁴⁵ and Sett *et al.*⁴⁷. This vibration is substituent sensitive and difficult to distinguish from ring in-plane deformation.

Natural bond orbital analysis (NBO): Natural bond orbital analysis provides an efficient method for studying intra- and intermolecular bonding and interaction among bonds. It also provides a convenient basis for investigating charge transfer or conjugative interaction in molecular systems. Some electron donor orbitals, acceptor orbitals and the interacting stabilization energy resulted from the second-order micro-disturbance theory are reported^{48,49}. The lowering of orbital energy due to the interaction between the doubly occupied orbital and the unoccupied ones is a very convenient guide to interpret the molecular structure. In energetic terms, hyperconjugation is an important effect in which an occupied Lewis-type natural bond orbital is stabilized by overlapping with a non-Lewis-type orbital. This electron delocalization can be described as a charge transfer from a Lewis valence orbital (donor), with a decreasing of its occupancy, to a non-Lewis orbital (acceptor). The larger the $E(2)$ value, the more intensive is the interaction between electron donors and electron acceptors, *i.e.* the more donating tendency from electron donors to electron acceptors and greater the extent of conjugation of the whole system. This interaction results in a loss of occupancy from the concentration of electron natural bond orbital of the idealized Lewis

(bond or lone pair) structure into an empty (*anti*-bond or Rydberg) non-Lewis orbital. Natural bond orbital analysis has been performed on the 2-benzoyl thiophene at the DFT/B3LYP/6-311++G** level in order to elucidate the intra-molecular hydrogen bonding, rehybridization and delocalization of electron density within the molecule. The second-order perturbation theory analysis of Fock matrix in natural bond orbital analysis of the title compounds shows strong intra-molecular hyperconjugative interactions are presented in Table-4. The intermolecular hyperconjugative interactions are formed by the orbital overlap between $\pi(\text{C-C})$, $\pi^*(\text{C-C})$ and $\sigma(\text{C-C})$, $\sigma^*(\text{C-C})$ bond orbitals, which results in ICT, causing stabilization of the system. These interactions are observed as an increase in the electron density (ED) in the C-C *anti*-bonding orbital that weakens the respective bonds. The electron density at the conjugated π bonds (1.65–1.8e) and π^* (bonds (0.31–0.34e) in the benzene and thiophene ring of the molecule indicate strong π delocalization within the rings. The electron density at the conjugated σ bonds ($\sim 1.98e$) and σ^* ($\sim 0.02e$) of the aromatic rings clearly demonstrates weak delocalization. The interactions in thiophene ring is between the lone pair of electrons present on S atom and the *anti*-bonding π orbital of the nearby conjugated bonds $\pi^*(\text{C1-C2}, \text{C3-C4})$. Also an exchange interaction among the bonding and anti-bonding π orbital of C1-C2 and C3-C4 ($E(2) = 16.10, 17.54 \text{ kcal/mol}$) further delocalizes the charge on the hetero aromatic ring. The interactions $\pi(\text{C7-C8}) \rightarrow \pi^*(\text{C9-C10}, \text{C11-C12})$, $\pi(\text{C9-C10}) \rightarrow \pi^*(\text{C7-C8}, \text{C11-C12})$ and $\pi(\text{C11-C12}) \rightarrow \pi^*(\text{C7-C8}, \text{C9-C10})$ are responsible for the conjugation of the respective π bonds in the benzene ring with a maximum stabilization up to $\sim 21 \text{ kcal/mol}$. The strong intramolecular hyperconjugative interaction of the π electrons from C1-C2, C7-C8 to the π^* *anti*-bonding orbital of C6-O13 bond shows an electron density of $\sim 1.7 e$, leading to the stabilization of 19.13 and 15.44 kcal/mol respectively. This enhanced $\pi^*(\text{C6-O13})$ natural bond orbital further conjugates with $\pi^*(\text{C7-C8})$ of the benzene ring resulting in an enormous stabilization energy of 117.34 kcal/mol. This interaction reveals the conjugation of the carbonyl group with the π system. The hyperconjugative interactions of the $\sigma \rightarrow \sigma^*$ transitions occur from various bonds in the molecules. The important interaction energy, related to the resonance in the molecule, are the natural bond orbital interactions of $n_2(\text{O13}) \rightarrow \sigma^*(\text{C1-C6}, \text{C6-C7})$ which leads to moderate stabilization energies of 19.73 and 18.41 kcal/mol respectively. The $n_1(\text{O13}) \rightarrow \sigma^*(\text{C1-C6}, \text{C6-C7})$ transitions are less stabilized with 1.67 and 1.99 kcal/mol respectively.

Mulliken atomic charges: Mulliken charges render net atomic populations in a molecule and has an important influence on the vibrational spectra⁵⁰. The Mulliken atomic charges calculated at the B3LYP/6-311++G** method are given in Table-5. The oxygen and sulphur have negative charge and all hydrogen atoms have net positive charge. The carbon Mulliken charges are found to be either positive or negative depending upon the nature of the atoms bonded to them. Since negative charge is located at the S atom of the thiophene ring the C1 and C4 carbon attached to this hetero-atom are found to be more negatively charged. The carbon atom C1 has the maximum positive charge of about 0.767e. Moreover

TABLE-4
SECOND ORDER PERTURBATION THEORY ANALYSIS OF FOCK MATRIX IN
NATURAL BOND ORBITAL BASIS FOR 2-BENZOYL THIOPHENE

Donor (i)	Electron density (i) (e)	Acceptor (j)	Electron density (j) (e)	E (2) ^a (Kcal mol ⁻¹)	E(j)-E(i) ^b (a.u)	F(i,j) ^c (a.u)
$\sigma(C_1-C_2)$	1.98013	$\sigma^*(C_1-C_6)$	0.06413	3.20	1.16	0.055
		$\sigma^*(C_2-C_3)$	0.01268	2.12	1.26	0.046
$\pi(C_1-C_2)$	1.79578	$\pi^*(C_3-C_4)$	0.30081	16.10	0.28	0.062
		$\pi^*(C_6-O_{13})$	0.19445	19.13	0.29	0.067
$\sigma(C_1-S_5)$	1.97815	$\sigma^*(C_2-H_{14})$	0.01574	3.40	1.15	0.056
		$\sigma^*(C_4-H_{16})$	0.01255	2.74	1.14	0.050
		$\sigma^{**}(C_6-O_{13})$	0.01039	1.77	1.24	0.042
$\sigma(C_1-C_6)$	1.98276	$\sigma^*(C_1-C_2)$	0.01876	3.21	1.26	0.057
$\sigma(C_3-C_4)$	1.98671	$\sigma^*(C_2-C_3)$	0.01268	2.21	1.27	0.047
$\pi(C_3-C_4)$	1.83385	$\pi^*(C_1-C_2)$	0.32648	17.54	0.30	0.067
$\sigma(C_4-S_5)$	1.98133	$\sigma^*(C_1-C_6)$	0.06413	3.55	1.12	0.057
		$\sigma^*(C_3-H_{15})$	0.01499	3.90	1.15	0.060
$\sigma(C_6-O_{13})$	1.99295	$\sigma^*(C_1-S_5)$	0.03417	1.90	1.25	0.044
$\pi(C_6-O_{13})$	1.96650	$\pi^*(C_1-C_2)$	0.32648	3.92	0.38	0.038
		$\pi^*(C_7-C_8)$	0.36563	3.86	0.40	0.038
$\pi(C_7-C_8)$	1.64541	$\pi^*(C_6-O_{13})$	0.19445	15.44	0.27	0.060
		$\pi^*(C_9-C_{10})$	0.31932	18.87	0.28	0.066
		$\pi^*(C_{11}-C_{12})$	0.29208	19.40	0.29	0.068
$\pi(C_9-C_{10})$	1.65381	$\pi^*(C_7-C_8)$	0.36563	21.33	0.28	0.070
		$\pi^*(C_{11}-C_{12})$	0.29208	18.16	0.29	0.065
$\pi(C_1-C_2)$	1.65501	$\pi^*(C_7-C_8)$	0.36563	19.39	0.28	0.066
		$\pi^*(C_9-C_{10})$	0.31932	21.24	0.28	0.069
$v_1(S_5)$	1.98383	$\sigma^*(C_1-C_2)$	0.01876	1.93	1.23	0.044
		$\sigma^*(C_3-C_4)$	0.01569	2.07	1.23	0.045
$v_2(S_5)$	1.62172	$\pi^*(C_1-C_2)$	0.32648	19.39	0.27	0.066
		$\pi^*(C_3-C_4)$	0.30081	22.78	0.26	0.071
$v_1(O_{13})$	1.97845	$\sigma^*(C_1-C_6)$	0.06413	1.67	1.12	0.039
		$\sigma^*(C_6-C_7)$	0.06318	1.99	1.12	0.043
$v_2(O_7)$	1.88248	$\sigma^*(C_1-S_5)$	0.03417	1.17	0.45	0.021
		$\sigma^*(C_1-C_6)$	0.06413	19.73	0.70	0.106
		$\sigma^*(C_6-C_7)$	0.06318	18.41	0.69	0.102
$\pi^*(C_6-O_{13})$	0.19445	$\pi^*(C_7-C_8)$	0.36563	117.34	0.01	0.064

^aE(2) means energy of hyper conjugative interactions; ^bEnergy difference between donor and acceptor I and j natural bond orbital orbitals.

^cF(i,j) is the Fock matrix element between i and j natural bond orbital orbital.

TABLE-5
MULLIKEN ATOMIC CHARGES OF 2-BENZOYL
THIOPHENE WITH THE B3LYP/6-311++G**

Atoms	Mulliken charges	Atoms	Mulliken charges
C ₁	0.767	C ₁₂	0.169
C ₂	0.587	O ₁₃	-0.216
C ₃	-0.843	H ₁₄	0.185
C ₄	0.234	H ₁₅	0.159
S ₅	-0.268	H ₁₆	0.261
C ₆	-1.984	H ₁₇	0.188
C ₇	1.615	H ₁₈	0.175
C ₈	-0.621	H ₁₉	0.163
C ₉	-0.418	H ₂₀	0.173
C ₁₀	-0.249	H ₂₁	0.213
C ₁₁	-0.294	-	-

the H21 and H16 atoms accommodate higher positive charge than the other hydrogen atoms. The presence of large value of negative charge on S and O and higher positive charge on H15 and H16 suggest the formation of intramolecular interactions. The theoretical non-bond distances C12H21...O13 (2.536 Å) and C4H16...S5(2.446 Å) also confirms this non bonded interaction.

Molecular electrostatic potential (MEP): Molecular electrostatic potential (MEP) maps are often used for the qualitative interpretation of electrophilic and nucleophilic reactions and the calculation of atomic charges^{51,52}. The molecular electrostatic potential surface (MEPS) is a method of mapping electrostatic potential on to the iso-electron density surface simultaneously displays electrostatic potential (electron + nuclei) distribution, molecular shape, size and dipole moments of the molecule and it provides a visual method to understand the relative polarity. The total electron density and MEPS of the molecules under investigation are constructed by using B3LYP/6-311++G** method. Molecular electrostatic potential mapping is very useful in the investigation of the molecular structure with its physiochemical property relationships. They use colour to portray the calculated electron distribution in a molecule. The different values of the electrostatic potential at the MEPS are represented by different colours; red, blue and green represent the regions of most negative, most positive and zero electrostatic potential, respectively. The negative (red and yellow) regions of MEPS are related to electrophilic reactivity and the positive (blue) regions to nucleophilic reactivity.

The electron total density onto which the electrostatic potential surface has been mapped is shown in Fig. 5. The negative regions are mainly localized on the oxygen atom of the benzoyl group with a maximum value of $V(r)$ as -0.05369 a.u. So it is predicted that an electrophile would preferentially attack 2-benzoyl thiophene around the O13 atom. The region of zero potential envelops the π system of the aromatic rings, leaving a more electrophilic region in the plane of hydrogen atoms. The most possible site for electrophilic attack is on H16 atom, which has a maximum positive $V(r)$ value of $+0.02738$ a.u.

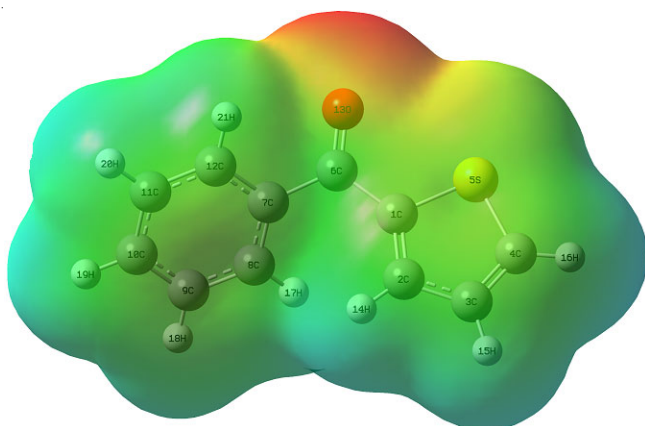


Fig. 5. Molecular electrostatic potential map of 2-benzoyl thiophene

Thermodynamic properties: The thermodynamic properties like heat capacity, entropy, rotational constants, dipole moment and zero point vibrational energy (ZPVE) of the title compound have also been computed at DFT-B3LYP level using 6-311++G** basis set and they are presented in Table-6. The measure of net molecular polarity is called the dipole moment. When the centers of gravity of the electrons and nuclei in a molecule don't coincide, the molecule possesses permanent dipole moment. Dipole moment values give information on inductive effects, shapes of molecules, hydrogen bonding, *etc.* The dipole moment of 2-benzoyl thiophene is found out to be 2.7144D. On the basis of vibrational analysis, the statically thermodynamic functions: standard entropies (S_m^0), standard heat capacities ($C_{p,m}^0$) and standard enthalpy changes (ΔH_m^0) for the title molecules are obtained from the theoretical harmonic frequencies are listed in Table-7. It can be observed that these thermodynamic functions are increasing with temperature ranging from 100 to 1000 K due to the fact that the molecular vibrational intensities increase with temperature. The correlation equations between heat capacity, Gibb's free energy, entropy, enthalpy changes and temperatures are fitted by quadratic formulas. The correlation graphs are shown in Fig. 6 and the corresponding fitting equations are as follows:

$$S_m^0 = 56.75433 + 0.16611T - 3.57803 \times 10^{-5} T^2 \quad (R = 0.9999)$$

$$C_{p,m}^0 = 1.01983 + 0.16352T - 7.03523 \times 10^{-5} T^2 \quad (R = 0.9988)$$

$$\Delta H_m^0 = -1.6395 + 0.01849T + 4.33902 \times 10^{-5} T^2 \quad (R = 0.9994)$$

Frontier molecular orbitals (FMOs): The concepts of aromaticity, HOMO and LUMO are of fundamental importance in understanding the chemical stability and reactivity of many organic molecules. Molecular orbital and their properties

TABLE-6
THEORETICALLY COMPUTED ZERO POINT VIBRATIONAL ENERGY (kcal mol^{-1}), ROTATIONAL CONSTANTS (GHz), ROTATIONAL TEMPERATURE (K), THERMAL ENERGY (kcal mol^{-1}), MOLAR CAPACITY AT CONSTANT VOLUME ($\text{cal mol}^{-1} \text{K}^{-1}$) ENTROPIES ($\text{cal mol}^{-1} \text{K}^{-1}$) AND DIPOLE MOMENT (Debye) FOR 2-BENZOYL THIOPHENE

Parameters	2-Benzoyl thiophene
Zero point vibration energy	99.13333
Rotational constants	1.69571 0.44729 0.36986
Rotational temperature	0.08138 0.02147 0.01775
Energy	
Translational	0.889
Rotational	0.889
Vibrational	103.912
Total	105.689
Molar capacity at constant volume	
Translational	2.981
Rotational	2.981
Vibrational	34.583
Total	40.544
Entropy	
Translational	41.600
Rotational	31.416
Vibrational	29.888
Total	102.904
Dipole moment	2.7144

TABLE-7
THERMODYNAMIC PROPERTIES AT DIFFERENT TEMPERATURES AT THE B3LYP/6-311++G** LEVEL FOR 2-BENZOYL THIOPHENE

Temp. (K)	Entropy (S) cal/mol-Kelvin	Heat capacity (Cp) cal/mol-Kelvin	Enthalpy (ΔH_m) kcal/mol
100.00	73.01	18.03	1.29
200.00	88.77	29.27	3.63
298.15	102.90	42.53	7.15
300.00	103.17	42.78	7.23
400.00	117.27	55.52	12.16
500.00	130.83	66.05	18.26
600.00	143.64	74.41	25.30
700.00	155.63	81.03	33.08
800.00	166.81	86.38	41.46
900.00	177.25	90.78	50.33
1000.00	187.00	94.44	59.59

like energy are very useful to the physicists and chemists and their frontier electron density is used for predicting the most reactive position in π electron system and also explains several types of reaction in conjugated systems⁵³. Both HOMO and LUMO are the main orbitals which take part in chemical stability. HOMO represents the ability to donate an electron, LUMO as an electron acceptor, represents the ability to obtain an electron. Moreover, eigen values of the HOMOs (π donor) and the LUMOs (π acceptor) and their energy gap reflects the chemical activity. The energy gap between HOMO and LUMO has been used to prove the bioactivity from intra-molecular charge transfer (ICT)⁵⁴. The conjugated molecules are characterized by HOMO–LUMO separation, which is the result of a

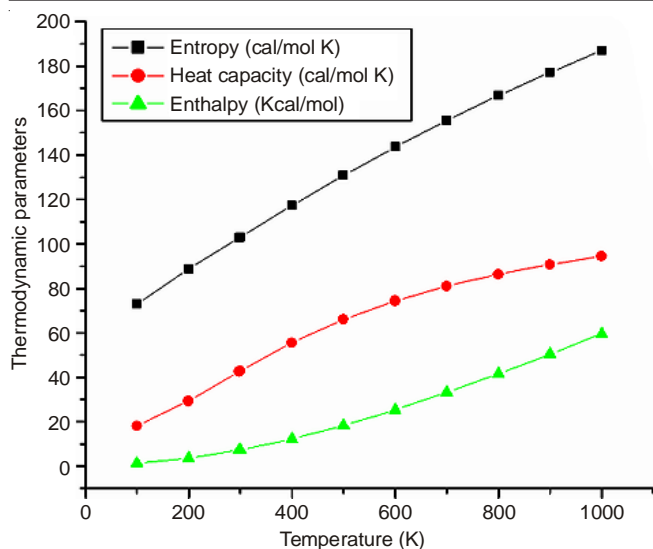


Fig. 6. Correlation of entropy, heat capacity and enthalpy with temperature of 2-benzoyl thiophene

significant degree of inter-molecular charge transfer from the end-capping electron-donor to the efficient electron acceptor group through π conjugated path. The strong charge transfer interaction through conjugated bridge results in substantial ground state donor-acceptor mixing and the appearance of a charge transfer band in the electronic absorption spectrum. Therefore, an electron density transfer occurs from the more aromatic part of the π conjugated system in the electron-donor side to electron-withdrawing part. The pictorial representation of the frontier molecular orbitals of 2-benzoyl thiophene are shown in Fig. 7. Molecular orbitals, when viewed in a qualitative graphical representation, can provide insight into the nature of reactivity and some of the structural and physical properties of molecules. Well known concepts such as conjugation, aromaticity and lone pairs are well illustrated by molecular orbitals. The energies of HOMO, LUMO orbitals of the compound are -0.2566, -0.0832 a.u. respectively. The HOMO-LUMO energy gap of 2-benzoyl thiophene calculated at DFT-B3LYP methods using 6-311++G** is 0.1733 a.u. The molecular orbitals of 2-benzoyl thiophene show that the electron density in the HOMO is mostly centered on the C=C of the thiophene ring, oxygen of the carbonyl group and partially over the benzene ring while in LUMO the electron density is predominantly located throughout the molecule. By using HOMO and LUMO energy values for a molecule, the global chemical reactivity descriptors of molecules such as hardness, chemical potential, softness, electronegativity and electrophilicity have been defined^{55,56}. According to Koopman's theorem, the energies of the HOMO and the LUMO orbital's of the molecule are related to the ionization potential (I) and the electron affinity (A), respectively, by the following relations: $I = -E_{\text{HOMO}}$ and $A = -E_{\text{LUMO}}$. As for the chemical hardness (η) is concerned, it is strongly associated with chemical stability and reactivity, the molecules with a small energy gap are known as soft and with large energy gap are termed as hard molecules. The hard molecules are highly stable and less reactive than the soft ones because it needs higher energy for its molecular excitation. The electronegativity (χ) and electrophilicity index (ω) have been understood as the power of an atom in a molecule to

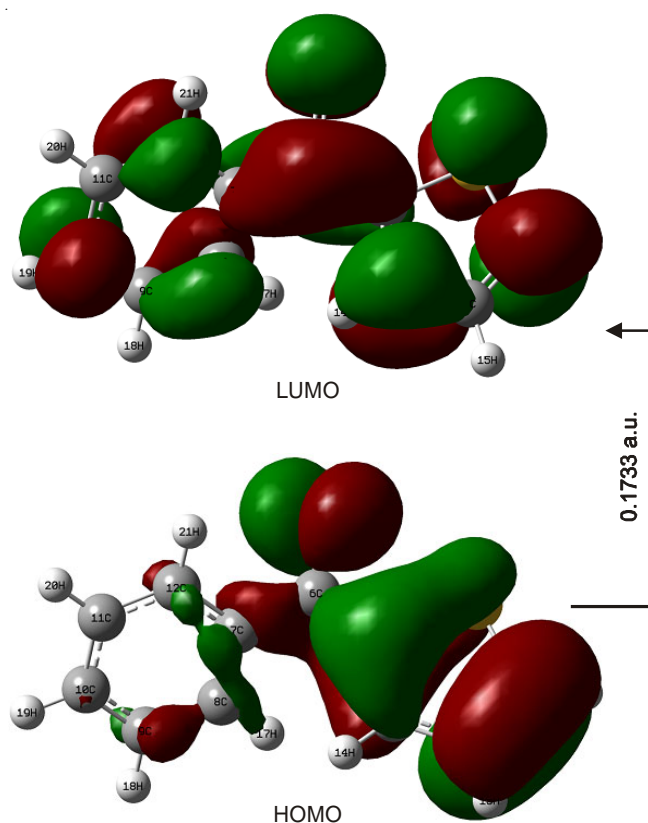


Fig. 7. Frontier molecular orbitals of 2-benzoyl thiophene

attract electrons and the capacity of the species to accept them. The hardness and electronegativity values of a molecule can be described to a good approximation from Koopman theorem as, $\eta = (I - A)/2$ and $\chi = (I + A)/2$. The softness is the inverse of the hardness $\sigma = 1/\eta$. The chemical potential that measures the escaping tendency of electron cloud is given by $\mu = -\chi$. The global electrophilicity index (ω) which measures the stabilization energy has been given by the following expression in terms of electronic chemical potential and the chemical hardness as $\omega = \mu^2/2\eta$ by Parr *et al.*⁵⁷. The quantum chemical parameters of the molecules are presented in Table-8.

TABLE-8
QUANTUM CHEMICAL PARAMETERS OF 2-BENZOYL
THIOPHENE CALCULATED AT B3LYP/6-311++G**

Chemical parameter	2-Benzoyl thiophene
Ionization potential (I) (a.u.)	0.24225
Electron affinity (A) (a.u.)	0.06851
Global hardness (η) (a.u.)	0.08687
Global softness (σ) (a.u.)	11.511454
Chemical potential (μ) (a.u.)	-0.15538
Electrophilicity (ω) (a.u.)	0.138960
Electro negativity (χ) (a.u.)	0.15538

Conclusion

A complete vibrational analysis of 2-benzoyl thiophene is performed by DFT-B3LYP method at 6-311++G** basis set level. The optimized molecular structure of the stable conformer, thermodynamic and electronic properties, vibrational frequencies, intensity of vibrations of the 2-benzoyl thiophene have been calculated by DFT method using B3LYP/6-

311++G** basis set. The theoretical results are compared with the experimental vibrations. On the basis of agreement between the calculated and experimental results, assignments of all the fundamental vibrational modes of the title compound are made unambiguously based on the results of the potential energy distribution output obtained from normal coordinate analysis. DFT calculation predicts two stable conformers. The carbonyl oxygen and the sulfur atom of the thiophene ring *syn* to each other, is the preferred conformation in 2-benzoyl thiophene, the S,O-*anti* conformation being less stable from S,O-*syn* by 7 kJ mol⁻¹. The stability of the molecule arising from hyperconjugative interaction and charge delocalizations have been analyzed using natural bond orbital analysis. Molecular electrostatic potential surface map shows regions around O13 and H16 atoms, the most possible site for nucleophilic and electrophilic attack. The lowering of the HOMOLUMO energy gap value has substantial influence on the intramolecular charge transfer of the molecule.

REFERENCES

1. T. Eicher, S. Hauptmann and A. Speicher, *The Chemistry of Heterocycles*; Wiley-VCH: New York, Ch. 5, Section 5.6 (2003).
2. K. Doré, S. Dubus, H.-A. Ho, I. Lévesque, M. Brunette, G. Corbeil, M. Boissinot, G. Boivin, M.G. Bergeron, D. Boudreau and M. Leclerc, *J. Am. Chem. Soc.*, **126**, 4240 (2004).
3. A.Kh. Sharipov, *Chem. Technol. Fuels Oil*, **38**, 340 (2002).
4. G. Rassu, F. Zanardi, L. Battistini and G. Casiraghi, *Chem. Soc. Rev.*, **29**, 109 (2000).
5. K.E. Schulze, P.R. Cohen and B.R. Nelson, *Dermatol. Surg.*, **32**, 407 (2006).
6. T.B.H. McMurry, *DNA Repair*, **6**, 1161 (2007).
7. C. Siebert and D. Das Bioisosterie-Konzept, *Chem. Unserer Zeit*, **38**, 320 (2004).
8. R.K. Russell, J.B. Press, R.A. Rampulla, J.J. McNally, R. Falotico, J.A. Keiser, D.A. Bright and A. Tobia, *J. Med. Chem.*, **31**, 1786 (1988).
9. K.I. Molvi, M. Mansuri, V. Sudarsanam, M.M. Patel, S.M.A. Andrabi and N. Haque, *J. Enzyme Inhib. Med. Chem.*, **23**, 829 (2008).
10. M.K. Parai, G. Panda, V. Chaturvedi, Y.K. Manju and S. Sinha, *Bioorg. Med. Chem. Lett.*, **18**, 289 (2008).
11. W. Wardakhan, O. Abdel-Salam and G. Elmegeed, *Acta Pharm.*, **58**, 1 (2008).
12. H.J. Chen, W.L. Wang, G.F. Wang, L.P. Shi, M. Gu, Y.D. Ren, L.F. Hou, P.L. He; F.H. Zhu, X.G. Zhong, W. Tang, J.P. Zuo and F.J. Nan, *ChemMedChem*, **3**, 1316 (2008).
13. A. Mongevega, J. Aldana, M.M. Rabbani and E. Fernandez-Alvarez, *J. Heterocycl. Chem.*, **17**, 77 (1980).
14. A.O. Abdelhamid and E.K.A. Abdelall, *J. Heterocycl. Chem.*, **46**, 680 (2009).
15. A.A. Sagaroy, M.J. Gil, R. Villar, M.J. Viñas, A. Arrazola, I. Encío and V. Martínez-Merino, *Bioorg. Med. Chem.*, **18**, 5701 (2010).
16. A.A. Fadda, E. Abdel-Latif and R.E. El-Mekawy, *Eur. J. Med. Chem.*, **44**, 1250 (2009).
17. X.M. Wu, X.S. Wu and J.Y. Xu, *J. Chin. Pharm. Univ.*, **27**, 641 (1996).
18. A.D. Burnett, A.M. Caplen, R.H. Davis Jr., R.E. Burrier and J.W. Clader, *J. Med. Chem.*, **37**, 1733 (1994).
19. A.K. Ansary and H.A. Omar, *Bull. Faculty Pharm.*, **39**, 17 (2001).
20. M.J. Frisch, G.W. Trucks, H.B. Schlegel, G.E. Scuseria, M.A. Robb, J.R. Cheeseman, J.A. Montgomery Jr., T. Vreven, K.N. Kudin, J.C. Burant, J.M. Millam, S.S. Iyengar, J. Tomasi, V. Barone, B. Mennucci, M. Cossi, G. Scalmani, N. Rega, G.A. Petersson, H. Nakatsuji, M. Hada, M. Ehara, K. Toyota, R. Fukuda, J. Hasegawa, M. Ishida, T. Nakajima, Y. Honda, O. Kitao, H. Nakai, M. Klene, X. Li, J.E. Knox, H.P. Hratchian, J.B. Cross, V. Bakken, C. Adamo, J. Jaramillo, R. Gomperts, R.E. Stratmann, O. Yazyev, A.J. Austin, R. Cammi, C. Pomelli, J.W. Ochterski, P.Y. Ayala, K. Morokuma, G.A. Voth, P. Salvador, J.J. Dannenberg, V.G. Zakrzewski, S. Dapprich, A.D. Daniels, M.C. Strain, O. Farkas, D.K. Malick, A.D. Rabuck, K. Raghavachari, J.B. Foresman, J.V. Ortiz, Q. Cui, A.G. Baboul, S. Clifford, J. Cioslowski, B.B. Stefanov, G. Liu, A. Liashenko, P. Piskorz, I. Komaromi, R.L. Martin, D.J. Fox, T. Keith, M.A. Al-Laham, C.Y. Peng, A. Nanayakkara, M. Challacombe, P.M.W. Gill, B. Johnson, W. Chen, M.W. Wong, C. Gonzalez and J.A. Pople, Gaussian, Inc., Wallingford CT (2004).
21. T. Sundius, *J. Mol. Struct.*, **218**, 321 (1990).
22. T. Sundius, *Vib. Spectrosc.*, **29**, 89 (2002).
23. P. Pulay, G. Fogarasi, G. Pongor, J.E. Boggs and A. Vargha, *J. Am. Chem. Soc.*, **105**, 7037 (1983).
24. G. Rauhut and P. Pulay, *J. Phys. Chem.*, **99**, 3093 (1995).
25. G. Keresztury, S. Holly, G. Besenyei, J. Varga, A. Wang and J.R. Durig, *Spectrochim. Acta A*, **49**, 2007 (1993).
26. G. Keresztury, J.M. Chalmers and P.R. Griffith, *Raman Spectroscopy: Theory in Handbook of Vibrational Spectroscopy*, vol. 1, John Wiley & Sons Ltd., New York (2002).
27. B.M. Craven and F.L. Ballas, *Acta Cryst.*, **B55**, 375 (1999).
28. M. Govindarajan and M. Karabacak, *Spectrochim. Acta A*, **96**, 421 (2012).
29. E.D. Simandiras, N.C. Handy and R.D. Amos, *J. Phys. Chem.*, **92**, 1739 (1988).
30. M. Kofranek, T. Kovár, H. Lischka and A. Karpfen, *J. Mol. Struct. THEOCHEM*, **259**, 181 (1992).
31. V. Balachandran, V. Janaki and A. Nataraj, *Spectrochim. Acta A*, **118A**, 321 (2014).
32. C.S. Chidan Kumar, C. Parlak, H.-K. Fun, M. Tursun, G. Kesan, S. Chandraru and C.K. Quah, *Spectrochim. Acta A*, **127**, 67 (2014).
33. K. Chaitanya, *Spectrochim. Acta A*, **86**, 159 (2012).
34. G. Mahalakshmi and V. Balachandran, *Spectrochim. Acta A*, **124A**, 328 (2014).
35. G. Varyansi, *Assignment for Vibrational Spectra of Seven Hundred Benzene Derivatives*, Akadémiai Kiadó, Budapest, vols. 1–2 (1973).
36. G. Socrates, *Infrared and Raman Characteristics Group Frequencies*, Wiley, New York, edn 3 (2001).
37. Y. Sert, L.M. Singer, M. Findlater, H. Dogan and C. Cirak, *Spectrochim. Acta A*, **128A**, 46 (2014).
38. L.J. Bellamy, *The Infrared Spectra of Complex Molecules*, Wiley, New York (1959).
39. C.N.R. Rao, *Chemical Application of Infrared Spectroscopy*, Academic Press, New York (1981).
40. M. Karabacak, S. Bilgili, T. Mavis, M. Eskici and A. Atac, *Spectrochim. Acta A*, **115A**, 709 (2013).
41. X.-H. Li and X.-Z. Zhang, *Spectrochim. Acta A*, **105**, 280 (2013).
42. N.B. Colthup, S.E. Wiberly and L.H. Daly, *Introduction to Infrared and Raman Spectroscopy*, Academic Press, New York (1990).
43. T.M. Kolev and B.A. Stamboliyska, *Spectrochim. Acta A*, **56**, 119 (2000).
44. G. Mahalakshmi and V. Balachandran, *Spectrochim. Acta A*, **124**, 328 (2014).
45. R.B. Viana, E.D.A. Santos, L.J. Valencia, R.M. Cavalcante, E.B. Costa, R. Moreno-Fuquen and A.B.F. da Silva, *Spectrochim. Acta A*, **102**, 386 (2013).
46. N.P.G. Roges, *A Guide to the Complete Interaction of Infrared Spectra of Organic Structures*, Wiley, New York (1994).
47. P. Sett, T. Misra, S. Chattopadhyay, A.K. De and P.K. Mallick, *Vib. Spectrosc.*, **44**, 331 (2007).
48. A.E. Reed, R.B. Weinstock and F. Weinhold, *J. Chem. Phys.*, **83**, 735 (1985).
49. A.E. Reed and F. Weinhold, *J. Chem. Phys.*, **78**, 4066 (1983).
50. R.S. Mulliken, *J. Chem. Phys.*, **23**, 1833 (1955).
51. P. Politzer and D.G. Truhlar, *Chemical Applications of Atomic and Molecular Electronic Potentials*, Plenum Press, New York (1981).
52. S.R. Cox and J. Williams, *Comput. Chem.*, **2**, 304 (1981).
53. K. Fukui, T. Yonezawa and H. Shingu, *J. Chem. Phys.*, **20**, 722 (1952).
54. B. Kosar and C. Albayrak, *Spectrochim. Acta A*, **78**, 160 (2011).
55. R.G. Parr, L. Szentpaly and S. Liu, *J. Am. Chem. Soc.*, **121**, 1922 (1999).
56. P.K. Chattaraj, B. Maiti and U. Sarkar, *J. Phys. Chem. A*, **107**, 4973 (2003).
57. R.G. Parr and P.K. Chattaraj, *J. Am. Chem. Soc.*, **113**, 1854 (1991).